Giménez, JB.; Martí, N.; Bouzas, A.; Ferrer, J.; Seco, A. (2020). A mathematical approach to predict the solids concentration in anaerobic membrane bioreactos (AnMBR): Evaluation of the volatile solids solubilization. Journal of Environmental Management. 271:1-8. https://doi.org/10.1016/j.jenvman.2020.110983

A MATHEMATICAL APPROACH TO PREDICT THE SOLIDS CONCENTRATION IN ANAEROBIC MEMBRANE BIOREACTOS (AnMBR): EVALUATION OF THE VOLATILE SOLIDS SOLUBILIZATION.

Juan B. Giménez[a*], Nuria Martí[b], Alberto Bouzas[b], José Ferrer[a], Aurora Seco[b].

[a]Institut Universitari d'Investigació d'Enginyeria de l'Aigua i Medi Ambient, IIAMA, Universitat Politècnica de València, Camí de Vera s/n, 46022 Valencia, Spain (e-mail: *juagiga5@iiama.upv.es; jferrer@hma.upv.es*)

[b]Departament d'Enginyeria Química, Escola Tècnica Superior d'Enginyeria, Universitat de València, Avinguda de la Universitat s/n, 46100 Burjassot, Valencia, Spain (e-mail: *nuria.marti@uv.es*; *alberto.bouzas@uv.es; aurora.seco@uv.es*)

Abstract

Anaerobic Membrane Bioreactors (AnMBR) are gaining attention as a suitable approach for sustainable low-strength wastewater treatment, as they bring together the advantages of both anaerobic treatments and membrane bioreactors. However, increasing the sludge retention time (SRT) necessary to favor hydrolysis increases the suspended solids concentration potentially leading to decreased permeate flux. Therefore, the availability of a mathematical approach to predict the solids concentration within an AnMBR can be very useful. In this work, a mathematical model

* Corresponding Author: tel. +34 96 354 30 85, e-mail: *juagiga5@iiama.upv.es*

describing the volatile solids concentration within the reactor as a function of the operating parameters and the influent characteristics is developed. The solubilization of organic particulates was clearly influenced by temperature and the SRT, whereas the hydraulic retention time influence was negligible. Furthermore, the activation energy value of about 20 kJ·mol^{-1} confirms the idea that diffusion of hydrolytic enzymes from the bulk solution to the particle surface is the rate-limiting step of hydrolysis.

Keywords: Particulates hydrolysis, mathematical modelling, solubilization constant, solids prediction, AnMBR.

1. INTRODUCTION.

The current trend in wastewater management is moving towards the development of sustainable technologies aimed to reclaim both water and resources (i.e. nutrients and energy) from wastewater (Daigger, 2008; Kleerebezem and van Loosdrecht, 2007; Larsen et al., 2009; Li and Yu, 2011). Anaerobic treatment is regarded as one of the most attractive options for the development of sustainable wastewater treatment systems, since they have the potential to both being net energy producers and enabling nutrients to be recovered whilst reducing the excess-sludge production (Chen, 2020).

Nevertheless, anaerobic treatment of Municipal wastewater (MWW) streams requires an efficient biomass retention method. Otherwise, the combination of typical high flow-rates and low Chemical Oxygen Demand (COD) concentrations on MWW, and the low growth rates of organisms carrying out anaerobic degradation of organic matter at moderate temperatures (medium latitude temperate climates) would result in prohibitive reaction volumes to maintain the required sludge retention time (SRT).

Anaerobic membrane bioreactors (AnMBR) exhibit an outstanding capacity for particulate matter retention, enabling AnMBR to efficiently decouple hydraulic

46 retention time (HRT) from SRT. However, one important issue in the design of MBR-
47 based systems is particles, since it affects the performance of the membrane.
48 Hydrolysis of particulate organic material has been considered the rate-limiting step
49 in anaerobic digestion (Nabi et al., 2020, 2019; Pavlostathis and Giraldo-Gomez, 1991),
50 although some authors have emphasized that the hydrolytic process still remains as the
51 least well-defined step (Gavala et al., 2003; Miron et al., 2000). The general kinetic
52 term of hydrolysis encompasses disintegration, solubilization and enzymatic hydrolysis
53 processes in most of the practical cases presented in literature (Batstone et al., 2002a).
54 Furthermore, hydrolysis rates decline with temperature (Lettinga et al., 2001), requiring
55 longer SRTs for hydrolysis to occur at sub-mesophilic temperatures. However,
56 increasing the SRT, while keeping the HRT constant, increases the suspended solids
57 concentration, potentially leading to decreased permeate flux (Smith et al., 2012).
58 Therefore, an accurate prediction of the solids concentration might be very useful to
59 achieve a proper AnMBR operation.
60 In spite of the complexity of anaerobic processes, mechanistic-modelling based on
61 the understanding of underlying biological processes is nowadays a well-stablished
62 modelling approach (Batstone et al., 2015; Robles et al., 2018). Furthermore, most of
63 the empirical/ semi-empirical modelling approaches tackling the physical process (i.e.
64 filtration) can accurately reproduce the sludge effect over the membrane performance.
65 However, these models use parameters requiring specific laboratory procedures and
66 equipment (e.g. SMP), that might result in continuity issues when interfaced to a given
67 biological model (Robles et al., 2013). Conversely, some authors (Ludwig et al., 2012;
68 Robles et al., 2013; Sarioglu et al., 2012) are developing new models easily combinable
69 with biological models, using the most critical variables to membrane fouling as model
70 parameters (i.e., shear intensity and solids concentration).

This work aims at describing a mathematical approach to predict the solids concentration within AnMBR, depending on the operating conditions. A 700-days period, during which the system performance was evaluated under different operating conditions, was used in order to fit the experimental data to the model prediction. A non-linear regression was used to estimate the volatile-solids solubilization constant to assess its variability with the operating conditions.

2. MATERIALS AND METHODS.

2.1. Demonstration-scale plant description.

The present work was carried out in a demonstration-scale plant placed in the "Barranco del Carraixet" wastewater treatment plant (WWTP), in Alboraya (Valencia), Spain. The demonstration-scale plant was fed with the effluent of the pre-treatment (grease and sand removal) of the full-scale WWTP. The AnMBR mainly consisted of a 1.3 m^3 jacketed anaerobic reactor connected to two 0.8 m^3 membrane tanks. Each membrane tank included one commercial ultrafiltration hollow-fiber membrane system (PURON®, Koch Membrane Systems, 0.05 µm pore size, 30 m^2 total filtering area). A rotofilter with a screen size of 0.5 mm was installed as pre-treatment. One equalization tank (0.3 m^3) and one Clean-In-Place tank (0.2 m^3) were also included as main elements of the pilot plant. A fraction of the produced biogas (0.5 Nm^3 per cubic meter of reactor volume) was continuously recycled to the anaerobic reactor in order to improve the stirring conditions and to favor the stripping of the produced gases from the liquid phase, whereas another fraction of the produced biogas (0.2-0.3 Nm^3/h per m2 of membrane) was also continuously recycled to the bottom of the hollow-fiber membranes in order to minimize the cake layer formation. Also, a degassing vessel was installed between each membrane tank and the corresponding vacuum pump to recover the bubbles of biogas in the permeate. A temperature control system was also

implemented, consisting of a warm-water tank equipped with a 6 kW resistance and a thermostat switch that maintained the water temperature at 65 ºC. The temperature in the anaerobic reactor was effectively controlled by a water pump that enabled the warm water to flow through the reactor jacket depending on the difference between the reactor temperature and the set point.

Figure 1 shows a general view (a), as well as a process flow diagram (b) of the demonstration-scale plant. Further details on the demonstration-scale plant components and operation can be found in Giménez et al. (2011).

a)

b)

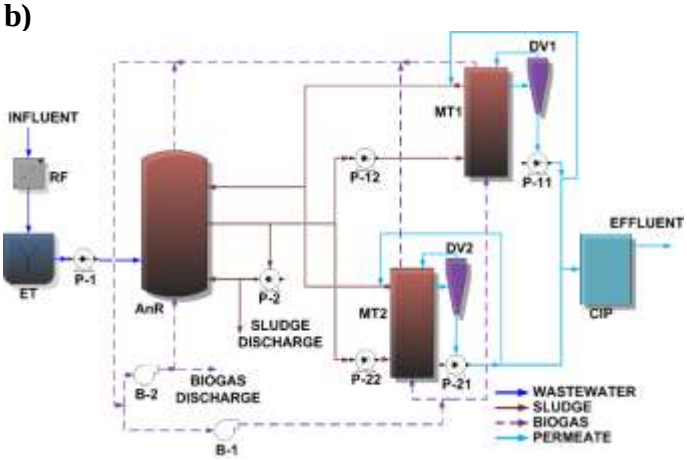

Figure 1. (a) General view and (b) Process Flow Diagram of the AnMBR demonstration plant. RF: Rotofilter; ET; Equalization Tank; AnR: Anaerobic Reactor; B: Blower; P: Pump; MT: Membrane Tank; DV: Degassing Vessel; CIP: Clean-In-Place.

2.2. Volatile Suspended Solids mass balance.

The general form of the volatile solids mass balance can be written according to Equation 1:

$$(Q_{WS} \cdot [VS]_R + Q_E \cdot [VS]_E) - Q_I \cdot [VS]_I + V_R \cdot \frac{d[VS]_R}{dt} = V_R \cdot \rho_H \qquad \text{Equation 1}$$

Where Q_{WS}, Q_E and Q_I are the waste sludge, effluent and influent volumetric flow rates, respectively. $[VS]_R$, $[VS]_E$ and $[VS]_I$ stand for the volatile-solids concentration in the reactor, effluent and influent, respectively. V_R is the volume of the reactor and ρ_H stands for the hydrolysis rate. The hydrolysis process of particulate organic matter encompasses several stages (i.e., enzyme production, diffusion, adsorption, reaction and enzymatic deactivation). However, first order kinetics are the most widespread in order to describe the hydrolysis process, since more complex kinetic equations only provide slightly better results (Batstone et al., 2002a). Therefore, the hydrolysis kinetics can be described by Equation 2:

$$\rho_H = k_H \cdot [SS_{BD}] \qquad \text{Equation 2}$$

Where $[SS_{BD}]$ stands for the biodegradable suspended solids concentration (mg $SS \cdot L^{-1}$), and k_H is the first order hydrolysis constant (day^{-1}) that encompasses the cumulative effect of every single process involved in the overall enzymatic hydrolysis process. The rate of hydrolysis depends on pH, temperature, concentration of hydrolyzing biomass and characteristics of particulates (Pavlostathis and Giraldo-Gomez, 1991). In order to set the volatile solids mass balance out, the following assumptions have been made:

1. Biodegradable suspended solids are comprised within the volatile suspended solids (VSS) fraction.
2. The dissolved fraction of the volatile solids is negligible as compared to the suspended fraction. Therefore, $[VSS] \cong [VS]$.
3. The biodegradable fraction of the volatile solids is constant during each period.

Therefore, according to assumption 1, a change in the biodegradable suspended solids will induce the same change in the VSS, so it is possible to rewrite the hydrolysis rate expression as in Equation 3:

$$\rho_H = k_H \cdot [SS_{BD}] \equiv k_H \cdot [VSS_{BD}] \equiv k_H \cdot f_{BD} \cdot [VSS] \quad \text{Equation 3}$$

f_{BD} standing for the biodegradable fraction of the volatile solids within the reactor. Therefore, considering assumption 2 and 3, the hydrolysis rate can be expressed as in Equation 4:

$$\rho_H \cong k_H \cdot f_{BD} \cdot [VS] \equiv k_{Sol,VS} \cdot [VS] \quad \text{Equation 4}$$

$k_{Sol,VS}$ being (Equation 5):

$$k_{Sol,VS} = k_H \cdot f_{BD} \quad \text{Equation 5}$$

Equation 4 states that the hydrolysis rate can be described as a function of the VS concentration within the reactor. The proportionality factor, the so-called VS solubilization constant ($k_{Sol,\,VS}$), encompasses both the first order hydrolysis constant and a factor that stands for the biodegradable fraction of the volatile solids. The hydrolysis constant reflects the cumulative effect of every step involved in the complete enzymatic hydrolysis process (enzyme production, diffusion, adsorption, reaction and deactivation; (Batstone et al., 2002a)) which has been reported to be a function of pH, temperature, hydrolytic biomass concentration and physio-chemical features of the substrate, among other parameters (Pavlostathis and Giraldo-Gomez, 1991), whereas the biodegradable fraction of the volatile solids depends on the biodegradable particulates accumulated within the reactor. Indeed, both parameters will depend on the influent MWW features, as well as on the selected operating conditions.

The resulting general expression for the volatile solids mass balance in continuous stirred tank reactors (CSTR) is given by Equation 6:

$$(Q_{WS} \cdot [VS]_R + Q_E \cdot [VS]_E) - Q_I \cdot [VS]_I + V_R \cdot \frac{d[VS]_R}{dt} = V_R \cdot \rho_H \equiv V_R \cdot k_{Sol,VS} \cdot [VS]_R \quad \text{Equation 6}$$

152 A further development of the VS and non-volatile solids (NVS) mass balances in
153 AnMBR, where $[VS]_E$ is negligible, resulted in Equation 7 and Equation 8 for the
154 estimation of the VS and NVS concentration within the reactor, respectively:

$$[\boldsymbol{VS}]_{\boldsymbol{R}} = -\frac{[VS]_I \cdot SRT}{(k_{Sol,VS} \cdot SRT - 1) \cdot HRT} + \left([VS]_R^0 + \frac{[VS]_I \cdot SRT}{(k_{Sol,VS} \cdot SRT - 1) \cdot HRT}\right) \cdot exp\left[\left(k_{Sol,VS} - \frac{1}{SRT}\right) \cdot t\right] \quad \text{Equation 7}$$

$$[\boldsymbol{NVS}]_{\boldsymbol{R}} = \frac{[NVS]_I \cdot SRT}{HRT} + \left([NVS]_R^0 - \frac{[NVS]_I \cdot SRT}{HRT}\right) \cdot exp\left[-\frac{t}{SRT}\right] \quad \text{Equation 8}$$

155 Where [NVS], HRT and SRT stand for the non-volatile solids concentration, the
156 hydraulic and the solids retention times, respectively. Subscripts have been used in the
157 same way than in Equation 1, whereas the superscript "0" has been used to denote the
158 concentration at the beginning of the considered period. Experimental data for $[VS]_I$,
159 $[NVS]_I$, $[NS]_R^0$ and $[NVS]_R^0$ in the different periods can be found in table S1 (support
160 material).

161 From the above expressions for the estimation of the VS and NVS concentration, it is
162 possible to estimate the VS percentage according to Equation 9:

$$\%\,VS_R = \frac{[VS]_R}{[TS]_R} \cdot 100 = \frac{[VS]_R}{[VS]_R + [NVS]_R} \cdot 100 \quad \text{Equation 9}$$

163 **2.3. Experimental design.**

164 The present work comprises 700 days of AnMBR demonstration plant operation that
165 was sub-divided into 10 different operating periods. HRT and SRT were easily
166 controlled by modifying the influent and waste-sludge flow-rates, respectively.

Temperature was controlled from period P1 to period P5, and in periods P9 and P10. Conversely, the temperature control was disconnected during periods P6 to P8, enabling the temperature of the system to evolve according to the ambient temperature. Table 1 shows the operating conditions that were set in each period.

Period	T (ºC)	HRT (h)	SRT (d)
P1	33	17	71
P2	33	12	71
P3	33	9	74
P4	33	6	71
P5	20	24	69
P6	29	28	42
P7	23	14	39
P8	17	12	29
P9	20	12	29
P10	20	12	40

Table 1. Operating conditions in the 10 periods evaluated.

2.4. Analytical methods.

Total solids (TS), Volatile solids (VS), Total suspended solids (TSS) and volatile suspended solids (VSS) for the influent and for the mixed liquor were determined according to Standard Methods (APHA et al., 2012).

3. RESULTS AND DISCUSSION.

3.1. Influence of the operating conditions over the VS solubilization process.

As previously stated, both the hydrolysis constant and the biodegradable fraction of the volatile solids depend on the influent MWW features, as well as on the selected operating conditions. Figure 2 (a) to (g) show the evolution of both the experimental (dots) and the estimated (lines) values for the VS and the NVS concentration during periods P1 to P5, P9 and P10.

(a) **(b)**

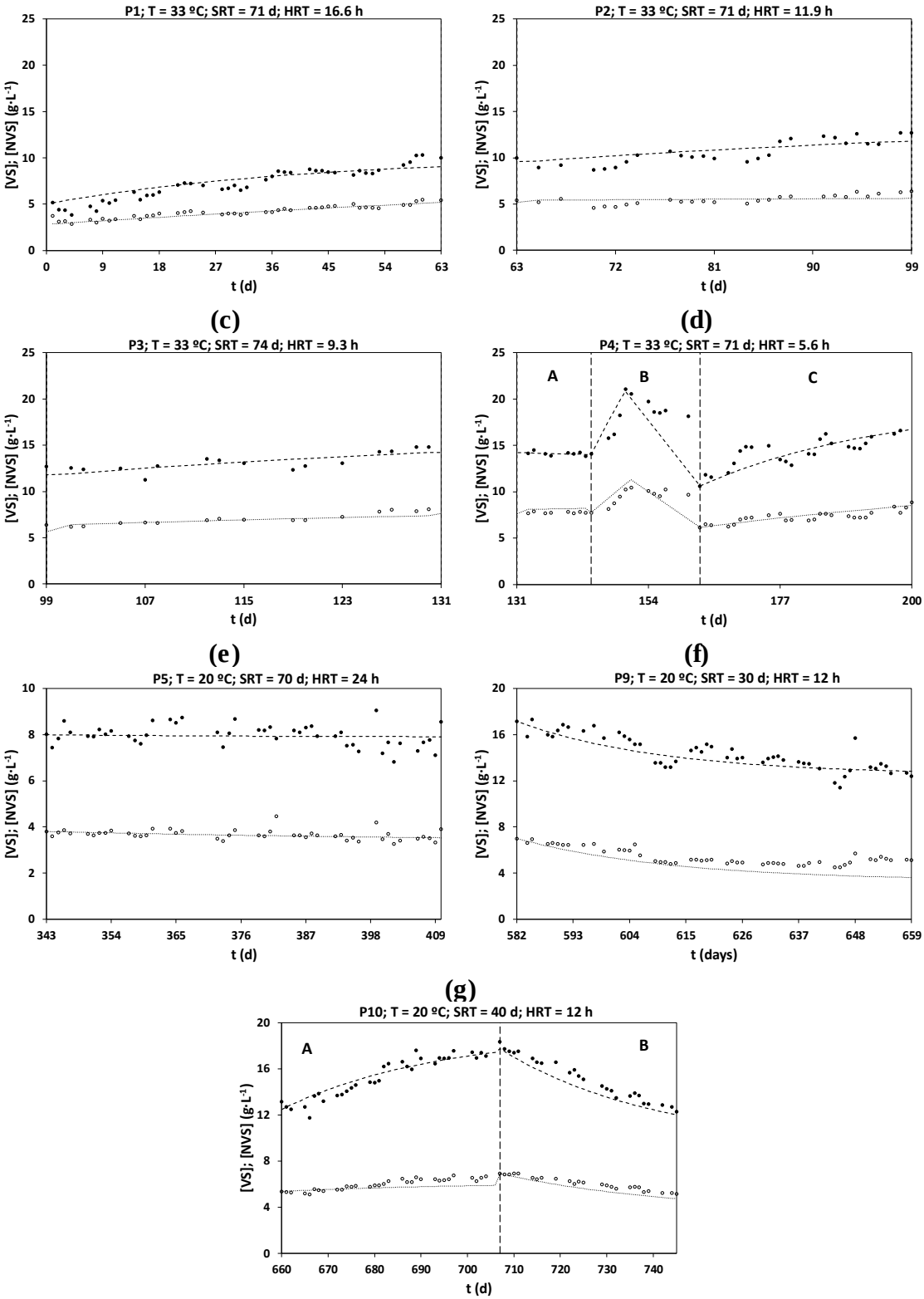

183 Figure 2 Time-evolution of the experimental and fitted Volatile solids [VS] and the Non-Volatile solids
184 [NVS] concentration.

185 As it can be seen in Figure 2, the estimated NVS concentration ($[NVS]_{Estimated}$)

186 accurately followed the experimental NVS concentration ($[NVS]_{Experimental}$) trend,

187 indicating that the average influent NVS concentration-values ($[NVS]_I$; Table S1) used
188 in the NVS mass balance (Equation 8) were representative of the actual influent NVS
189 concentration during the different periods. Likewise, it can be assumed that the average
190 influent VS concentration values ($[VS]_I$; Table S1) were also representative of the actual
191 influent VS concentration during each period. Therefore, the VS mass balance
192 (Equation 7) was used to adjust the volatile-solids solubilization constant ($k_{Sol,VS}$) by
193 means of the least-squares, non-linear fitting of the estimated VS concentration data
194 ($[VS]_{Estimated}$), to the experimental data ($[VS]_{Experimental}$). An evaluation of the influence
195 of the operating conditions over $k_{Sol,VS}$ is presented below.

196 **3.1.1. Hydraulic Retention Time.**

197 In order to assess the effect of the HRT on the VS solubilization process, the VS
198 solubilization constant was estimated from the non-linear fitting of the VS balance
199 concentration data to the analytical VS concentration data during periods P1, P2, P3 and
200 P4. As shown in Table 1, SRT and temperature were set to 70 days and 33ºC,
201 respectively, whereas HRT was decreased from 17 to 6 hours. Table 2 shows the
202 estimated values for the VS solubilization constant during periods P1 to P4.

Period	HRT (h)	$k_{Sol,VS}$ (d^{-1})
P1	16.6	0.0186
P2	11.9	0.0068
P3	9.3	0.0067
P4	5.6	0.0181

203 Table 2. Variation of the Volatile Solids solubilization constant ($k_{Sol, VS}$) with HRT.

204 The VS solubilization constant was similar during periods P1 and P4, despite the
205 three-fold reduction in the HRT. These results evidenced the negligible influence of the
206 HRT over the hydrolysis process. On the other hand, the VS solubilization constants
207 during periods P2 and P3 were lower than for periods P1 and P4, the lowest value being
208 that of period P3.

209 The reduced VS solubilization constant during periods P2 and P3 was attributed to
210 the domestic-featured influent wastewater, given that P2 and P3 corresponded to the
211 summer period, in which the industrial fraction of wastewater is significantly reduced.
212 Indeed, a clear difference in the organic load and composition of the influent wastewater
213 was observed between summer and the rest of the year (Giménez, 2014), indicating that
214 the biodegradability of the domestic fraction of the MWW was lower than the industrial
215 fraction. These results suggest that it was the different influent wastewater features
216 during summer rather than the HRT what influenced the volatile-solids solubilization
217 constant $k_{Sol,VS}$, by means of the likely different volatile solids biodegradable fraction in
218 the reactor (f_{BD}).

219 **3.1.2. Temperature.**

220 Previous works (Giménez et al., 2014, 2012) have reported a clear influence of
221 temperature on the volatile solids percentage within AnMBR, indicating an uneven
222 solubilization of the volatile solids as a result of the hydrolysis-rate variation with
223 temperature. Additionally, the variation in the hydrolysis rate affected the availability of
224 substrates in the subsequent stages of the anaerobic degradation. Indeed, transitory VFA
225 accumulation was observed at the beginning of period P5 (data not shown), which was
226 attributed to the acetogenic and methanogenic unbalanced activities derived from the
227 temperature change, rather than from the change in the hydrolysis rate. During these
228 transitory impaired methanogenic-activity periods the high retention capacity of the
229 membranes helped to wash the VFA out of the system, preventing the AnMBR
230 acidification (reactor pH was virtually constant). The eventual depletion of VFA
231 indicated that the balance between the different microbial communities was restored,
232 and that hydrolysis was again the limiting step in the anaerobic degradation of organic
233 matter. Thus, both the biogas and waste sludge productions varied accordingly. In this

234 work, the influence of temperature variations over the VS solubilization process was
235 evaluated by comparing the VS solubilization constants estimated in periods P4 and P5.
236 The SRT was set at 70 days, whereas temperature was decreased from 33ºC, in period
237 P4, to 20 ºC, in P5. HRT was higher in period P5 than in period P4, however, the
238 solubilization process was not affected by this operating parameter, as previously
239 reported.

240 Figure 2 (d) and (e) shows the evolution of both the experimental (dots) and
241 estimated (dashed lines) values for the VS and NVS concentration during periods P4
242 and P5.

243 The estimated VS solubilization constant dropped by 26 % with the temperature
244 decrease, reducing its value from 0.0200 day^{-1} at 33 ºC (P4) to 0.0148 day^{-1} at 20 ºC
245 (P5). The data were fitted to a Van't Hoff-Arrhenius equation, given by the Equation
246 10:

$$k_{Sol,VS} = A \cdot e^{-\frac{E_a}{R \cdot T}} \qquad \text{Equation 10}$$

247 Where A stands for the pre-exponential factor (day^{-1}), E_a for the activation energy
248 ($kJ \cdot mol^{-1}$) and R being the universal gases constant (0.008314 $kJ \cdot mol^{-1} \cdot K^{-1}$). The
249 experimental data fitting resulted in the values for the Van't Hoff-Arrhenius parameters
250 shown in Equation 11:

$$k_{Sol,VS} = 17{,}78 \cdot e^{-\frac{17{,}28}{R \cdot T}} \qquad \text{Equation 11}$$

251 Veeken and Hamelers (1999) determined the activation energy for the hydrolysis of
252 4 selected bio-wastes (i.e. leaves, straw, orange peelings and grass). Hydrolysis
253 constants were determined using the non-linear, least-squares method to fit cumulative
254 methane production data to a first-order kinetics expression. Batch biomethane potential
255 tests were carried out at 20, 30 and 40 ºC, and it was assumed that hydrolysis was the
256 limiting step of the anaerobic digestion and that intermediary products were being

consumed as soon as they were produced. These authors attributed the accurate fitting of the first-order kinetic model to a total occupation of the enzyme adsorption sites by hydrolytic enzymes that were whether already present in the bio-waste component surface or rapidly produced by fast-growing hydrolytic microorganisms. The hydrolysis rates followed an Arrhenius-type behavior, resulting in an average activation energy in the order of 64 $kJ \cdot kmol^{-1}$, which is a typical value for enzyme kinetics, confirming that the enzyme concentration must have been exceeding the concentration of degradable surface-sites. Conversely, the results obtained in the present work for the Van't Hoff-Arrhenius equation parameters derived from the VS solubilization constants at 33 ºC and at 20 ºC, suggest that diffusion of hydrolytic enzymes from the bulk solution to the particle surface was rather the rate-limiting step of hydrolysis of MWW particulates, since the activation energy for diffusion is in the order of 20 $kJ \cdot mol^{-1}$. The observed difference was attributed to the combination of two factors. On the one hand, according to previous studies (Moñino et al., 2016), the average size of organic particulates in the MWW used in this study was more than a couple orders of magnitude lower (d_{50} = 0,0398 mm) than that of the bio-wastes used by Veeken and Hamelers (1999) in their study (5-10 mm), leading to a much higher concentration of enzyme adsorption sites. On the other hand, in continuous operation, hydrolytic enzymes must reach their adsorption site, regardless of the mechanism used (Batstone et al., 2002b), before the enzymatic reaction can take place. The combination of these two factors resulted in a shift of the hydrolysis limiting step towards enzyme diffusion rather than enzymatic reaction.

According to Tchobanoglous et al. (2003), if a rate coefficient is known at one temperature, it may be calculated at another (within the range over which the

281 temperature dependent coefficient rises with increases in temperature) by rearranging
282 the Arrhenius equation as shown in Equation 12:

$$k_{T_2} = k_{T_1} \cdot e^{\frac{E_a \cdot (T_2 - T_1)}{R \cdot T_1 \cdot T_2}} \quad \text{Equation 12}$$

283 Because the mesophilic temperature range is small when T is expressed in K, the
284 term ($R \cdot T_1 \cdot T_2$) in Equation 12 does not vary significantly and may be considered to be
285 constant. Therefore, Equation 12 can be rewritten as Equation 13:

$$k_{T_2} = k_{T_1} \cdot \theta^{(T_2 - T_1)} \quad \text{Equation 13}$$

286 Where θ is known as the temperature coefficient, and can be calculated by means of
287 Equation 14:

$$\theta = e^{\frac{E_a}{R \cdot T_1 \cdot T_2}} \quad \text{Equation 14}$$

288 In the present study, θ was found to be 1.0234, resulting in the temperature-
289 correction expression given by Equation 15:
290

$$k_{T_2} = k_{T_1} \cdot 1.0234^{(T_2 - T_1)} \quad \text{Equation 15}$$

291

292 **3.1.3. Sludge Retention Time.**

293 The influence of the SRT over the VS solubilization process was assessed during
294 periods P5, P9 and P10, during which the SRT was set to 70, 30 and 40 days,
295 respectively, and the temperature remained constant in 20 ºC. The HRT in P5 was
296 higher than in periods P9 and P10, however the influence of this operating parameter
297 was negligible, as previously reported.

298 Figure 2 (e) to (g) show the evolution of both the experimental (dots) and the
299 estimated (dashed lines) values for the VS and NVS concentrations during periods P5,
300 P9 and P10. Table 3 shows the estimated values for the VS solubilization constant

obtained from the non-linear fitting of the model to the analytical data during periods P5, P9 and P10.

Period	SRT (d)	$k_{Sol,VS}$ (d^{-1})
P5	70	0.0148
P10	40	0.0055
P9	30	0.0026

Table 3. Variation of the VS solubilization constant with SRT.

The values obtained for $k_{Sol,VS}$ in periods P5, P9 and P10, during which the SRT was set to 70, 30 and 40 days, respectively, indicate that the hydrolysis rate declined with the reduction of the SRT. These results stated that the influence of the SRT over the hydrolysis process was not only related to the extent of the hydrolysis achieved as a function of the contact time between the organic particulate matter and the enzymes carrying out the hydrolysis process within the reactor. In addition, the hydrolysis rate was also affected by the SRT, which was attributed to a shift in the hydrolytic activity. Indeed, previous studies demonstrated that an increase in the SRT entailed an increase in the relative abundance of some hydrolytic microorganisms (Durán et al., 2018). These results are in agreement with those reported by Veeken and Hamelers (1999), which indicated that the hydrolysis rate depends, among others, on the concentration of hydrolytic biomass.

Figure 3 shows the correlation between the SRT and the VS solubilization constant. A linear regression analysis was performed (see Table S2; support material), and the analysis of variance stated that there exists a statistically-significant linear correlation between both parameters within the range of SRT studied (P-value = 0.0083). Furthermore, the Pearson's correlation coefficient (r = 0.9999) indicated that the correlation was strong, with 99,98 % of the variability in $K_{Sol,VS}$ being explained by the model, as evidenced by the coefficient of determination (R^2).

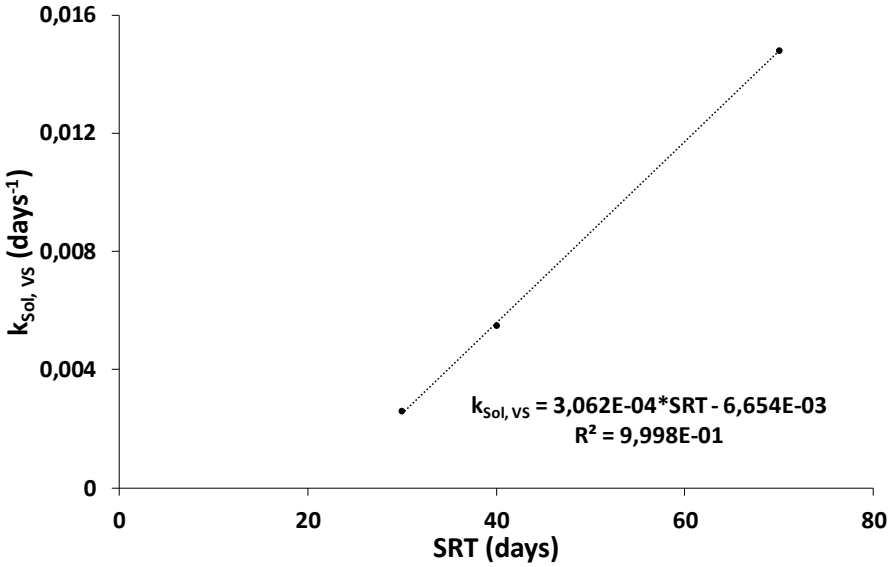

Figure 3. Correlation between $k_{Sol, VS}$ and SRT at 20ºC.

As stated in section 3.1.2, VFA accumulation was observed at the beginning of periods P5 (SRT = 70 days). It has been hypothesized that the VFA accumulation was attributed to a temperature decrease rather than to a hydrolysis-rate variation. Likewise, VFA accumulated at the beginning of period P9 (SRT = 30 days) in spite of the lower hydrolysis rate, confirming this hypothesis. Conversely, no VFA accumulation was observed during period P10 (SRT = 40 days), indicating that the balance between the different microbial groups was not affected by the enhanced hydrolysis derived from the SRT increase from period P9 to period P10. Alternatively, previous works (Giménez et al., 2014, 2012) reported that COD mass balances in the different periods indicated that the biogas and waste sludge productions were completely dependent on the hydrolysis extent, as long as hydrolysis was the limiting step.

3.2. Model Validation

Periods P6, P7 and P8 were used to validate the model prediction. To this aim, the volatile solids solubilization constants were calculated from the mathematical expression found for the influence of the SRT (see Figure 3). Experimental data used to

341 calibrate the influence of SRT were obtained during operation at 20 ºC. Therefore, the
342 calculated $k_{Sol,\,VS}$ were further corrected for temperature with equation 14. Table 4
343 shows the operating parameters set in each period and the estimations for the volatile
344 solids solubilization constant.

Period	T (ºC)	HRT (d)	SRT (d)	$k_{Sol,\,VS}$ (d^{-1})
P6	29	1.44	42	0.0078
P7	23	0.64	43	0.0071
P8	17	0.63	29	0.0021

345 Table 4. Operating conditions and kSol, VS estimated for periods P6, P7 and P8.

346 The time-course evolution for both the volatile and non-volatile solids concentration
347 in the reactor was compared to that predicted by Equation 7 and Equation 8,
348 respectively, using the $k_{Sol,\,VS}$ previously estimated.

349

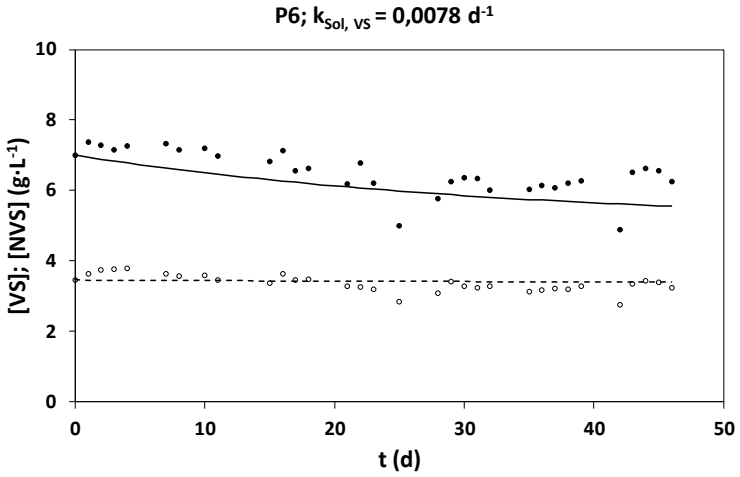

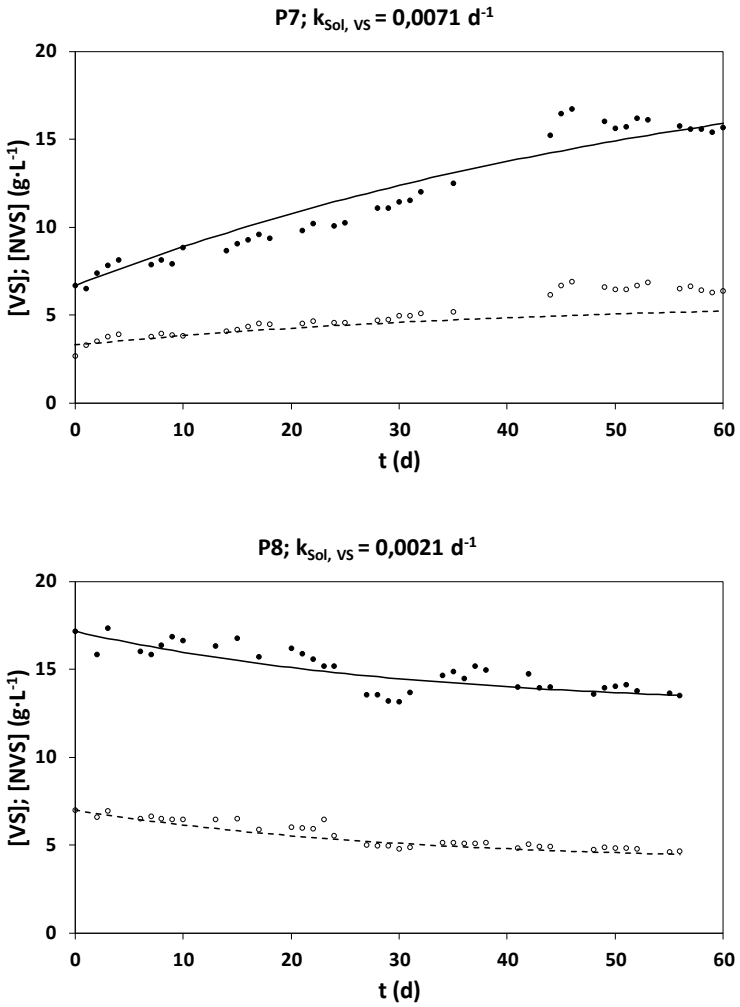

Figure 4. Model validation

Figure 4 shows the time-course evolution for both the experimental and the predicted volatile and non-volatile solids concentration values. This figure shows that the model calibration and further validation on the basis of experimental results allowed to accurately predict the volatile and non-volatile solids concentrations in an AnMBR treating real MWW, depending on the HRT, the SRT and the temperature of operation.

The applicability of the model is limited to specific MWW in the range of SRT and temperatures tested in this work. Nevertheless, it is worth of mention that the inclusion of additional parameters (e.g. biodegradable fraction of the volatile solids, f_{BD}) would enable to extend the applicability of the model to a wider range of influent characteristics. Furthermore, in spite of the wide knowledge regarding the effect of

361 temperature on the hydrolysis rate, additional operation data at different temperatures
362 could assist in the calculation of a more accurate Van't-Hoff- Arrhenius-equation
363 activation energy, which would be useful to determine the limiting stage of the
364 hydrolysis process in AnMBR treating MWW.

365 ## 4. CONCLUSIONS.

366 This work presents a mathematical approach to predict the solids concentration
367 within an AnMBR, depending on the influent wastewater characteristics and the
368 operating conditions.

369 The influence of the HRT on the VS solubilization was negligible, as evidenced by
370 the close values for the VS solubilization constant, despite the three-fold reduction of
371 the HRT. Therefore, lower $k_{Sol,VS}$ during summer periods were attributed to the different
372 influent wastewater features rather than to HRT.

373 The hydrolysis extent was higher with longer SRT, as a result of the extended contact
374 time between the organic particulate matter and the enzymes carrying out the hydrolysis
375 process. Furthermore, the shift in the relative abundance of hydrolytic microorganisms
376 with SRT also influenced the hydrolysis rate.

377 $k_{Sol,VS}$ decreased by 26 % with temperature decrease from 33 ºC to 20 ºC. Data fitting
378 to an Arrhenius equation resulted in an activation energy of 17,28 $kJ \cdot mol^{-1}$ suggesting
379 that diffusion of hydrolytic enzymes from the bulk solution to the adsorption site is the
380 rate-limiting step of hydrolysis.

381 The model calibration and further validation on the basis of experimental results
382 allowed to accurately predict the volatile and non-volatile solids concentrations in an
383 AnMBR treating real MWW, depending on the operating HRT, SRT and temperature.

ACKNOWLEDGEMENTS.

This research work was supported by the Spanish Research Foundation (CICYT) under Grants CTM2008-06809-C02-01 and CTM2008-06809-C02-02); Comunitat Valenciana Regional Government under Grant GVACOMP2009-285.

REFERENCES.

APHA, AWWA, WEF, 2012. Standard Methods for the Examination of Water & Wastewater.

Batstone, D.J., Keller, J., Angelidaki, I., Kalyuzhnyi, S.V., Pavlostathis, S.G., Rozzi, A., Sanders, W.T.M., Siegrist, H., Vavilin, V.A., 2002a. The IWA Anaerobic Digestion Model No 1 (ADM1), Water Science and Technology. IWA Publishing.

Batstone, D.J., Keller, J., Angelidaki, I., Kalyuzhnyi, S.V., Pavlostathis, S.G., Rozzi, A., Sanders, W.T.M., Siegrist, H., Vavilin, V.A., 2002b. Anaerobic Digestion Model No. 1.

Batstone, D.J., Puyol, D., Flores-Alsina, X., Rodríguez, J., 2015. Mathematical modelling of anaerobic digestion processes: applications and future needs. Rev. Environ. Sci. Bio/Technology 14, 595–613. https://doi.org/10.1007/s11157-015-9376-4

Chen, C., 2020. Anaerobic membrane bioreactors for sustainable and energy-efficient municipal wastewater treatment, in: Current Developments in Biotechnology and Bioengineering. pp. 335–366. https://doi.org/10.1016/B978-0-12-819852-0.00014-2

Daigger, G.T., 2008. New approaches and technologies for wastewater management, in: The Bridge. Vol. 38-2: Technologies for Clean Water. pp. 38–45.

Durán, F., Zamorano-López, N., Barat, R., Ferrer, J., Aguado, D., 2018. Understanding the performance of an AnMBR treating urban wastewater and food waste via model simulation and characterization of the microbial population dynamics. Process Biochem. 67, 139–146. https://doi.org/10.1016/j.procbio.2018.02.010

Gavala, H.N., Yenal, U., Skiadas, I. V., Westermann, P., Ahring, B.K., 2003. Mesophilic and thermophilic anaerobic digestion of primary and secondary sludge. Effect of pre-treatment at elevated temperature. Water Res. 37, 4561–4572. https://doi.org/10.1016/S0043-1354(03)00401-9

Giménez, J.B., 2014. Estudio del tratamiento anaerobio de aguas residuales urbanas en biorreactores de membranas. University of Valencia.

Giménez, J.B., Martí, N., Ferrer, J., Seco, A., 2012. Methane recovery efficiency in a submerged anaerobic membrane bioreactor (SAnMBR) treating sulphate-rich urban wastewater: Evaluation of methane losses with the effluent. Bioresour. Technol. 118, 67–72. https://doi.org/10.1016/j.biortech.2012.05.019

Giménez, J.B., Martí, N., Robles, A., Ferrer, J., Seco, A., 2014. Anaerobic treatment of urban wastewater in membrane bioreactors: Evaluation of seasonal temperature variations. Water Sci. Technol. 69, 1581–1588. https://doi.org/10.2166/wst.2014.069

Giménez, J.B., Robles, A., Carretero, L., Durán, F., Ruano, M. V, Gatti, M.N., Ribes, J., Ferrer, J., Seco, A., 2011. Experimental study of the anaerobic urban wastewater treatment in a submerged hollow-fibre membrane bioreactor at pilot scale. Bioresour. Technol. 102, 8799–806. https://doi.org/10.1016/j.biortech.2011.07.014

Kleerebezem, R., van Loosdrecht, M.C.M., 2007. Mixed culture biotechnology for bioenergy production. Curr. Opin. Biotechnol. 18, 207–12. https://doi.org/10.1016/j.copbio.2007.05.001

433 Larsen, T.A., Alder, A.C., Eggen, R.I.L., Maurer, M., Lienert, J., 2009. Source
434 Separation: Will We See a Paradigm Shift in Wastewater Handling? Environ. Sci.
435 Technol. 43, 6121–6125. https://doi.org/10.1021/es803001r
436 Lettinga, G., Rebac, S., Zeeman, G., 2001. Challenge of psychrophilic anaerobic
437 wastewater treatment. Trends Biotechnol. 19, 363–370.
438 https://doi.org/10.1016/S0167-7799(01)01701-2
439 Li, W.-W., Yu, H.-Q., 2011. From wastewater to bioenergy and biochemicals via two-
440 stage bioconversion processes: a future paradigm. Biotechnol. Adv. 29, 972–82.
441 https://doi.org/10.1016/j.biotechadv.2011.08.012
442 Ludwig, T., Gaida, D., Keysers, C., Pinnekamp, J., Bongards, M., Kern, P., Wolf, C.,
443 Sousa Brito, A.L., 2012. An advanced simulation model for membrane bioreactors:
444 Development, calibration and validation. Water Sci. Technol. 66, 1384–1391.
445 https://doi.org/10.2166/wst.2012.249
446 Miron, Y., van Lier, J.B., Lettinga, G., 2000. Miron 2000. Water Res. 34, 1705–1713.
447 Moñino, P., Jiménez, E., Barat, R., Aguado, D., Seco, A., Ferrer, J., 2016. Potential use
448 of the organic fraction of municipal solid waste in anaerobic co-digestion with
449 wastewater in submerged anaerobic membrane technology. Waste Manag. 56,
450 158–165. https://doi.org/10.1016/j.wasman.2016.07.021
451 Nabi, M., Zhang, G., Li, F., Zhang, P., Wu, Y., Tao, X., Bao, S., Wang, S., Chen, N.,
452 Ye, J., Dai, J., 2020. Enhancement of high pressure homogenization pretreatment
453 on biogas production from sewage sludge: a review. Desalin. Water Treat. 175,
454 341–351. https://doi.org/10.5004/dwt.2020.24670
455 Nabi, M., Zhang, G., Zhang, P., Tao, X., Wang, S., Ye, J., Zhang, Q., Zubair, M., Bao,
456 S., Wu, Y., 2019. Contribution of solid and liquid fractions of sewage sludge
457 pretreated by high pressure homogenization to biogas production. Bioresour.

458 Technol. 286, 121378. https://doi.org/10.1016/j.biortech.2019.121378
459 Pavlostathis, S.G., Giraldo-Gomez, E., 1991. Kinetics of anaerobic treatment: A critical
460 review. Crit. Rev. Environ. Control 21, 411–490.
461 https://doi.org/10.1080/10643389109388424
462 Robles, Á., Ruano, M.V., Charfi, A., Lesage, G., Heran, M., Harmand, J., Seco, A.,
463 Steyer, J., Batstone, D.J., Kim, J., Ferrer, J., 2018. A review on anaerobic
464 membrane bioreactors (AnMBRs) focused on modelling and control aspects.
465 Bioresour. Technol. 270, 612–626. https://doi.org/10.1016/j.biortech.2018.09.049
466 Robles, A., Ruano, M. V., Ribes, J., Seco, A., Ferrer, J., 2013. A filtration model
467 applied to submerged anaerobic MBRs (SAnMBRs). J. Memb. Sci. 444, 139–147.
468 https://doi.org/10.1016/j.memsci.2013.05.021
469 Sarioglu, M., Insel, G., Orhon, D., 2012. Dynamic in-series resistance modeling and
470 analysis of a submerged membrane bioreactor using a novel filtration mode.
471 Desalination 285, 285–294. https://doi.org/10.1016/j.desal.2011.10.015
472 Smith, A.L., Stadler, L.B., Love, N.G., Skerlos, S.J., Raskin, L., 2012. Perspectives on
473 anaerobic membrane bioreactor treatment of domestic wastewater: a critical
474 review. Bioresour. Technol. 122, 149–59.
475 https://doi.org/10.1016/j.biortech.2012.04.055
476 Tchobanoglous, G., Burton, F.L., Stensel, H.D., Metcalf & Eddy, I., Burton, F., 2003.
477 Wastewater Engineering: Treatment and Reuse, McGraw-Hill higher education.
478 McGraw-Hill Education.
479 Veeken, A., Hamelers, B., 1999. Effect of temperature on hydrolysis rates of selected
480 biowaste components. Bioresour. Technol. 69, 249–254.
481